

# Harnessing the strategy of metagenomics for exploring the intestinal microecology of sable (*Martes zibellina*), the national first-level protected animal

**Jiakuo Yan**

Qufu Normal University

**Xiaoyang Wu**

Qufu Normal University

**Jun Chen**

Ocean University of China

**Yao Chen**

Ocean University of China

**Honghai Zhang** (✉ [zhanghonghai67@126.com](mailto:zhanghonghai67@126.com))

Qufu Normal University

---

## Original article

**Keywords:** Sable (*Martes zibellina*) Metagenomics, Gut microbiota, Functional database, Gene function annotation

**Posted Date:** August 10th, 2020

**DOI:** <https://doi.org/10.21203/rs.3.rs-28506/v2>

**License:**   This work is licensed under a Creative Commons Attribution 4.0 International License.

[Read Full License](#)

---

**Version of Record:** A version of this preprint was published on September 18th, 2020. See the published version at <https://doi.org/10.1186/s13568-020-01103-6>.

# Abstract

Sable (*Martes zibellina*), belongs to *Carnivora*, *Mustelidae* and *Martes*, was mainly distributed among the cold northern zone of Eurasia. The purpose of this study is to explore the intestinal flora of the sable by the method of the metagenomic library-based technique, libraries were sequenced on an Illumina HiSeq 4000 instrument. Effective Data volume of each sample is above 6000M, the ratio of the Effective Data (the Clean Data) to original Data (Raw Data) is over 98%. According to the analysis of statistical data, the Total length of ORF is about 603,031, which is 347.36 Mbp. We contrast the unique function of genes with KEGG database, we acquire 7140 genes (KO), a total of all the samples KO is 129788. We selected higher abundance genes to draw cluster heat maps, and according to the results of the KEGG metabolic pathway annotations, we acquire the gene function—including metabolism, environmental information processing, genetic information processing, cellular process and organismal systems. We contrast the unique function of genes with CAZy database, the functional carbohydrate hydrolases have corresponding genes in the intestinal microorganisms of the sable. This is closely related to the fact that the sable is adapted to cold environments and requires a large amount of energy to maintain its metabolic activity. We contrast the unique function of genes with eggNOG database—the main functions of genes included gene duplication, recombination and repair, transport and metabolism of amino acids, transport and metabolism of carbohydrates, etc. In this study, we intended to identify the complex microbial population structure of sables based on metagenomic sequencing method, which uses the whole metagenomic data, mapping the sequences to the known genes or the pathways in the existing databases, such as CAZy, KEGG, or eggNOG, and then exploring the genetic composition and functional diversity of microbial community based on the mapped functional categories.

## Introduction

The communities of microorganism residing in the gastrointestinal (GI) tract of animals are vast and diverse, even outnumbering the number of host cells (Krone et al. 2014; Li et al. 2018a; Zhu et al. 2018). To some extent, intestinal microbial population could be considered a separate organ that encode 150-fold more genes than host genome (Guan et al. 2016; Hasan et al. 2019; Jain et al. 2018). In general, the gut microflora is considered a diverse and dynamic ecosystem that keeps homeostasis of the intestinal tract (Ma et al. 2019; Oliphant and Allen-Vercoe 2019; Taha-Abdelaziz et al. 2018). It has been discovered that the intestinal microbiota status is closely related to intrinsic and extrinsic factors including birth, diet, nutrition, stress, drugs, habitat and social contact (Hale et al. 2019; Jang et al. 2018; Li et al. 2017; Robertson et al. 2018). Nowadays, it is widely known that gut microorganisms are indispensable for the host nutrient absorption and metabolism (De Mandal et al. 2018; Deng et al. 2019; Dong et al. 2018; Pan et al. 2019; Si et al. 2020), for instance, *Firmicutes*, *Bifidobacterium*, and *Lactobacillus*, which have multiple beneficial effects on host metabolism to produce energy and short-chain fatty acids (SCFAs) (Antunes et al. 2019; Bang et al. 2018; Blakeley-Ruiz et al. 2019). Furthermore, the intestinal microbiota regulates carbohydrate and lipid metabolism (Li et al. 2018b; Pekkala et al. 2017), provide the host with source of energy or activate receptors (Federici 2019). It is worth mentioning that intestinal

microorganisms are involved in the synthesis of key vitamins that cannot be produced by the host organisms (Grieneisen et al. 2019; Martin et al. 2018; Srugo et al. 2019). Evidence has accumulated to show gut microbiota antigenic stimuli play a significant role in shaping the intestinal immune responses that can affect host overall health (Doulberis et al. 2015; Liu et al. 2019; Wu et al. 2017a; Xue et al. 2019). The intestinal bacteria is also related to the development of the intestinal epithelium to strengthen the intestinal barrier function (Hill et al. 2016; Li et al. 2019; Xu et al. 2020).

The sable (*Martes zibellina*), one of the species of carnivorous mammals, ranging across the cold northern zone of Eurasia (Li et al. 2013), is famous for its precious and thermal fur (Guan et al. 2016; Monakhov et al. 2018; Svishcheva and Kashtanov 2011). Sable has a slender body and a high surface-to-volume ratio which maintain a low body fat rate of about 8 percent even during particularly cold winters (Mustonen and Nieminen 2006), thus a high energy metabolic rate should be required for survival (Mustonen et al. 2006), so we decided to investigate the correlations of metabolism function with intestinal flora. Traditionally, the sort of microflora was determined through the methods of bacteria culture (Wu et al. 2017b). However, the growth environment of many bacteria cannot be replicated, which hinders the study of microbial diversity and function (Tully et al. 2018). In recent years, the progress of high-throughput sequencing technologies has been a fundamental advancement in DNA sequencing (Shui et al. 2020). With the declined expense of DNA sequencing, metagenomics has been in the stage of rapid development (Johnson 2019). The technique is usually used to sequence and analyze the whole genome of microbes in an entire sample, without the necessity for cell cultures, it is widely applied to probe environmental microbial diversity from the all levels, in consequence further study of the microbial community structure and ecosystem function is possible (Martin et al. 2018).

In this study, we sought to identify the complex microbial population structure of sables based on metagenomic sequencing method, which uses the whole metagenomic data, mapping the sequences to the known genes or the pathways in the existing databases, such as CAZy, KEGG, or eggNOG, and then exploring the genetic composition and functional diversity of microbial community based on the mapped functional categories. In ancient China, the sable was considered a precious fur animal, however, at present there was not mature rearing strategy. Given this, the work was devoted to acquire detailed views into the functional structure of intestinal flora and will provide valuable information to guide breeding for the sable.

## Materials And Methods

All fecal samples were collected from Dalian Mingwei Marten Industry Company Limited, these wild sables imported from Mohe County of Heilongjiang Province and Greater Khingan Range. According to carnivorous characteristics of the sable, they were fed fish and chicken. When collecting stool samples, we recorded the details of host gender, sample date and cage number. Fresh fecal samples from sables were collected aseptically in a sterile stool container, then all fecal samples were immediately frozen in the refrigerator. These samples were categorized into three groups: the five female sable fecal samples were named MZF.1–MZF.5, the four male sable fecal samples were named MZM.1–MZM.4, and

intestinal contents were named MZS.1, MZB.1 and MZB.2 (Table 1). Before DNA extraction from fecal samples, we guarantee the freshness of samples and reduce the pollution of the environment on the samples.

**Table 1 Table of the information in samples**

Species	Sample	Sex	Time
Sable	MZF.1	Female	2017.11
Sable	MZF.2	Female	2017.11
Sable	MZF.3	Female	2017.11
Sable	MZF.4	Female	2017.11
Sable	MZF.5	Female	2017.11
Sable	MZM.1	Male	2017.11
Sable	MZM.2	Male	2017.11
Sable	MZM.3	Male	2017.11
Sable	MZM.4	Male	2017.11
Sable	MZS.1	Male	2017.11
Sable	MZB.1	Male	2017.11
Sable	MZB.2	Male	2017.11

### **DNA extraction library preparation and metagenomics sequencing**

The QIAamp Fast DNA Stool Mini Kit (Qiagen, Hilden, Germany) was exploited to extract microbial DNA from the stool of sable. The detection of DNA samples mainly includes two methods. Agarose gel electrophoresis (AGE) was used to analyze the purity and integrity of DNA and Qubit 2.0 (Invitrogen, USA) quantified DNA concentrations precisely. During the library construction step, qualified DNA samples were randomly broken into a length of about 350 bp fragments with ultrasonic crusher (Covaris, UK), then the fragments were end-repaired, A-tailed, ligated to adapters. After the library preparation, Qubit 2.0 (Invitrogen, USA) was used for initial quantification and the library was diluted to 2 ng/μl. Subsequently, using Agilent 2100 Bioanalyzer (Agilent, USA) to detect if the insert sizes of the library correspond to expectations. In order to ensure the quality of library, Real-time q-PCR was used to accurately quantify the effective concentration (> 3 nM) of library. After the library passed the inspection, sequencing was

implemented on Illumina HiSeq xten platform (Illumina, USA). The raw reads are available at the NCBI Sequence Read Archive (BioProject ID PRJNA630144, SRA SRP265006).

## Quality control and genome assembly

After sequencing, raw genome data that contain adapter information and low-quality bases would interfere with the subsequent analysis. First of all, the original data should be controlled to remove interfering data to obtain clean data. There was the possibility of host genome contamination, which needs to be compared with the host gene database to filter out reads that may be host gene (SoapAligner parameter settings: identity  $\geq$  90%, -l 30, -v 7, -M 4, -m 200, -x 400). Reads with a quality value less than 38 (the default  $\leq$  40) and N (undetected bases) reached the set number (default set to 10) in the original data were removed. Remove reads that the overlap between adapter and the sequence exceeds a certain threshold ( $\geq$  15 bp). Clean Data was obtained after pretreatment, and the SOAP denovo assembly software was used for assembly analysis (Luo et al. 2012). For a single sample, k-mer = 55 was selected for assembly to obtain the assembly result of the sample (Assembly parameters: -d 1, -M 3, -R, -u, -F) (Brum et al. 2015; Feng et al. 2015; Qin et al. 2014; Scher et al. 2013). The Scaffolds were interrupted from the N-junction to obtain N-free sequence fragments, called Scaffigs (i.e., continuous sequences within scaffolds) (Mende et al. 2012). The Clean Data of each sample was compared to Scaffigs of each sample by SoapAligner software to obtain PE reads (Alignment parameters: -u, -2, -m 200). Put reads of each sample that had not been utilized together, and k-mer =55 was selected for mixed assembly (Karlsson et al. 2013), other assembly parameters are the same as single sample assembly parameters. The Scaffolds were broken from the N-junction to obtain the Scaffigs sequences without N. For Scaffigs generated by single sample and mixed assembly, fragments less than 500 bp were filtered out (Zeller et al. 2014), and statistical analysis and subsequent genetic prediction were performed.

## Gene prediction and abundance analysis

Starting from the Scaffigs of each sample and mixed assembly ( $\geq$ 500bp), MetaGeneMark was used for ORF (Open Reading Frame) prediction (Li et al. 2014), and fragments length less than 100nt were filtered from the prediction results. For the ORF prediction results of each sample, the CD-HIT software was used to remove redundancy, so as to obtain the initial gene catalogue with non-redundancy. Clustering is conducted with identity 95% and coverage 90%, and the longest sequence is selected as the representative sequence (parameters: -c 0.95, -G 0, -aS 0.9, -g 1, -d 0). The Clean Data of each sample was compared with the initial gene catalogue by SoapAligner, and the number of reads of genes in each sample was calculated (Alignment parameters: -m 200, -x 400, identity  $\geq$  95%). The number of genes supporting reads in each sample  $\leq$ 2 were filtered out to obtain the final gene catalogue for subsequent analysis (Qin et al. 2012). The abundance information of each gene in each sample was calculated from the number of reads and gene length (Villar et al. 2015). Based on the abundance information of each

gene in each sample, basic information statistics, core-pan gene analysis, correlation analysis between samples, and gene number Venn diagram analysis were conducted (blastp  $\text{evalue} \leq 1e-5$ ).

## Species annotation

DIAMOND software was used to compare unigenes with the sequences of Bacteria, Fungi, Archaea and Viruses extracted from NCBI NR database (Buchfink et al. 2015). Alignment filtering: for each sequence alignment,  $\text{evalue} \leq \text{minimum evalue} * 10$  is selected for subsequent analysis. After filtering, since there may be multiple alignment results for each sequence to obtain multiple different species classification information, in order to ensure its biological significance, LCA algorithm (systematic classification applied to MEGAN software) was adopted to take the classification level before the first branch as the species annotation information of the sequence (Huson et al. 2011). According to the LCA annotation results and gene abundance table, the abundance information of each sample at each classification level (genus and species) is obtained. The abundance of a species in a sample is equal to the sum of the gene abundance of the species annotated. Based on the LCA annotation results and gene abundance table, the gene number table of each sample at each classification level (genus and species) was obtained. For a species, the number of genes in a sample was equal to the number of genes whose abundance was not 0 in the annotated species.

## Functional database and resistance gene annotation

Currently, the commonly functional databases mainly include: Kyoto Encyclopedia of Genes and Genomes (KEGG), Evolutionary genealogy of genes: Non-supervised Orthologous Groups (eggNOG), Carbohydrate-Active enzymes Database (CAZy). KEGG database was introduced by Kanehisa Laboratories in 1995 with version 0.1. At present, it has developed into a comprehensive database, the core of which is KEGG pathway and KEGG Ortholog database. In the KEGG Ortholog database, genes performing the same function are clustered together and called Ortholog Groups (KO entries). In the KEGG pathway database, biological metabolic pathways are divided into 6 categories, which are Cellular Processes, Environmental Information Processing, Genetic Information Processing, Human Diseases, Metabolism, Organismal Systems, each of which is systematically classified as layer 2, 3, 4. The second layer currently includes 43 seed pathways, the third layer is the metabolic pathway diagram and the fourth layer is the specific annotation information of each metabolic pathway map. The database of eggNOG uses the smith-waterman comparison algorithm to annotate the Orthologous Groups of constructed genes. EggNOG V4.1 covers 2,031 species and about 190,000 Orthologous Groups are constructed. CAZy database is the study of carbohydrate enzyme professional database, mainly covers six functional categories: GHs (Glycoside Hydrolases), GTs (Glycosyl Transferases), PLs (Polysaccharide Lyases), CEs (Carbohydrate Esterases), AAs (Auxiliary Activities) and CBMs (Carbohydrate Binding Modules). DIAMOND software was used to compare Unigenes with each functional database (blastp,

evaluate  $\leq 1e-5$ ). Alignment filtering: for alignment results of each sequence, the alignment results with the highest score (one HSP > 60 bits) were selected for subsequent analysis. Based on the result of functional annotation and gene abundance table, the number of genes in each sample at each classification level is obtained. The number of genes with a certain function in a sample is equal to the number of genes with a non-zero abundance in the genes with a certain function. Based on the abundance table at each classification level, carry out annotation gene number statistics and relative abundance overview. Using the Resistance Gene Identifier (RGI) software provided by CARD to compare Unigenes with CARD database (RGI built-in blastp, evaluate  $\leq 1e-30$ ) (Qin et al. 2010). According to the comparison results of RGI and the abundance information of unigenes, the relative abundance of ARO was calculated. According to ARO abundance, circle diagram of abundance distribution, ARO difference analysis between groups, and species attribution analysis of resistance genes (note to ARO unigenes) were conducted.

## Results

### Extraction of total microbial DNA from samples

The microbial genomes of the samples were extracted using QIAGEN specialized kit for DNA extraction of stool samples, and the total DNA was preliminarily detected by agarose-gel electrophoresis, and the total DNA concentration was detected by Qubit Fluorometer to check whether the samples met the requirements for database construction. The results were shown in Table 2.

### Table 2 The detection report of DNA

Sample name	Concentration (ng/μl)	Volume (μl)	Total (ng)	Library type	Test Results
MZF.1	11.4	51	581	Meta	A
MZF.2	13	51	663	Meta	A
MZF.3	7.6	51	388	Meta	A
MZF.4	10	51	510	Meta	A
MZF.5	0.8	51	41	Meta	A
MZM.1	37	51	1887	Meta	A
MZM.2	5.7	51	291	Meta	A
MZM.3	16	51	816	Meta	A
MZM.4	2.54	51	130	Meta	A
MZS.1	7.2	51	367	Meta	A
MZB.1	4.7	51	240	Meta	A
MZB.2	21	51	1071	Meta	A

### Sequencing data statistics

Using Illumina HiSeq 4000 sequencing platform to get the original data (Raw data), the sequencing data was statistically analyzed. First of all, removing low quality reads from the original data to control the quality of the raw data. In total, after size filtering and quality control, with an average effective data of 6000 M for each sample was obtained. The clean data accounting for more than 98% of the raw data, showing that the valid data met the quality requirements for subsequent analysis. Specific statistical results are shown in Table 3.

**Table 3 The statistical information of sample data**

Sample	Raw Data	Clean Data	Clean_Q20	Clean_Q30	Clean_GC (%)	Effective (%)
MZF.1	6,423.43	6,348.62	97.36	95.16	52.27	98.835
MZF.2	6,400.51	6,371.69	97.28	95.07	49.81	99.55
MZF.3	6,337.84	6,290.67	97.46	95.33	51.35	99.256
MZF.4	6,792.60	6,769.70	97.12	94.95	41.59	99.663
MZF.5	6,390.60	6,341.12	96.89	95.33	45.32	99.226
MZM.1	6,272.72	6,260.54	97.11	94.76	47.25	99.806
MZM.2	7,024.25	7,010.36	96.72	94.53	38.97	99.802
MZM.3	6,252.62	6,230.76	97.25	95.01	50.56	99.65
MZM.4	6,612.68	6,556.58	95.95	94.00	41.27	99.152
MZS.1	6,438.21	6,360.45	96.71	94.22	42.41	98.792
MZB.1	6,266.57	6,244.48	96.58	94.82	47.00	99.648
MZB.2	6,809.10	6,693.22	96.75	91.59	47.48	98.298

### Valid data assembly results

After the quality control and filtering, the data are ready for assembling. Firstly, finding the overlap relationship between sequences based on sequence similarity, then we building Contig sequences based on overlap relationship. Furthermore, Scaffold sequence were obtained by connecting Contig sequence based on paired-end relationship. The gap still exists in the Scaffold sequence, it's usually denoted by N or n. Finally, the scaffold assembled was interrupted from the N connection to obtain the scaftig sequence fragment without N. We usually use NOVO\_MIX to filter out the Scaftigs fragments under 500bp. These sequences were used for subsequent analysis. The results of data assembly are shown in Table 4.

**Table 4 The statistical information of sample assembled results**

Sample	Total len. (bp)	Num.	Average len. (bp)	N50 Len. (bp)	Max len. (bp)
MZF.1	36,356,589	34,785	1,045.18	1,087	73,452
MZF.2	31,081,373	22,094	1,406.78	1,711	305,593
MZF.3	18,869,947	14,803	1,274.74	1,492	39,052
MZF.4	62,710,239	46,632	1,344.79	1,670	91,860
MZF.5	32,307,271	23,551	1,371.80	1,703	52,978
MZM.1	45,524,309	37,738	1,206.33	1,328	226,903
MZM.2	79,892,828	65,995	1,210.59	1,373	185,211
MZM.3	14,205,478	11,729	1,211.14	1,341	41,989
MZM.4	33,869,693	26,595	1,273.54	1,511	86,091
MZS.1	33,880,650	26,234	1,291.48	1,419	243,912
MZB.1	30,495,188	17,768	1,716.30	2,789	400,796
MZB.2	2,101,244	2,820	745.12	692	15,984
NOVO_MIX	205,647	273	753.29	700	5,562

## Gene prediction

After data assembly, MetaGeneMark was used to predict the open reading frames (ORFs). The predicted length less than 100nt will be filtered, then we use the CD - HIT software to get rid of the redundant information (protein level) and obtain the non-redundant initial gene catalogue. We usually choose identity 95% and coverage 90% for the clustering, the longest sequence was selected as the representative sequence. Next, the Clean Data of each sample was compared with the original gene catalogue using the SoapAligner software, the number of reads of the gene compared in each sample was obtained, the genes with reads less than or equal to 2 in each sample were filtered out. We got the distribution of reads in reference genes. Moreover, the abundance information of each gene in each sample was obtained. Based on the statistical data, we got ORF (Open Reading Frame) for a total of 603,031, the number of genes with both start codon and stop codon accounted for 29.38%~49.66% in each sample, the number of genes with neither initiation codon nor termination codon accounted for 5.83%~12.09%. The total length of ORF predicted was 347.36 Mbp, we usually use average length to indicate the ORF, the average length of each sample is shown in Table 5.

**Table 5 The statistical information of predicted gene**

Sample	ORFs NO	Integrity: none	Integrity: all	Total length	Average length
MZB.1	39,513	3,004(7.6%)	19,623(49.66%)	25.86	654.52
MZB.2	1,766	103(5.83%)	718(40.66%)	0.5	284.09
MZF.1	57,458	6,949(12.09%)	16,882(29.38%)	31.42	546.78
MZF.2	43,961	3,734(8.49%)	18,541(42.18%)	26.64	606
MZF.3	27,858	2,972(10.67%)	10,265(36.85%)	16.63	597.07
MZF.4	91,228	8,049(8.82%)	37,356(40.95%)	54.37	595.93
MZF.5	47,236	3,832(8.11%)	20,673(43.77%)	27.95	591.7
MZM.1	67,006	7,037(10.5%)	24,051(35.89%)	39.32	586.82
MZM.2	105,623	8,052(7.62%)	46,010(43.56%)	54.35	514.59
MZM.3	21,266	2,107(9.91%)	8,287(38.97%)	12.07	567.54
MZM.4	50,935	4,540(8.91%)	20,947(41.12%)	29.4	577.3
MZS.1	49,063	4,797(9.78%)	20,141(41.05%)	28.82	587.47
NOVO_MIX	118	4(3.39%)	57(48.31%)	0.03	234.56

## Species abundance

Based on the relative abundance table of different classification levels, the top 35 genera with abundance and their abundance information in each sample were selected to draw a heat map, and clustering was conducted at the level of species to facilitate the result display and information discovery, so as to identify the species with more aggregation in the sample (Fig.1).

Fig.1 Cluster heat map of relative abundance at genus level

To show the relative abundance of intestinal flora more intuitively, according to the intestinal flora data, boxplot denote the relative abundance of gut bacterial at the phylum taxonomical level. At the phylum level, *Firmicutes* and *Proteobacteria* were the preponderant phylum in all groups (Fig.2).

Fig.2 Relative abundance of gut bacterial at the phylum taxonomical level

## Principal Component Analysis

Because of the complexity of sample data, we used Principal Component Analysis (PCA) to reduce and simplify the sample data. Results from principal component analysis (PCA) are shown in Fig. 3.

Fig.3 Principal Component Analysis

## KEGG annotation results

The predicted Unique Genes were compared with the KEGG functional database, and 7140 genes (KO) were obtained. The total number of genes (KO) in all samples reached 127,839. As shown in Figure 4, the number of genes related to carbohydrate metabolism was the highest, accounting for 11.86%, which proves that carbohydrate, as the most important energy supplier, is the main energy source provided to the host by intestinal flora in Environmental information. Among the processing functions, the number of genes related to membrane transportation is high proportion, accounting for 7.79% of the total number of genes in all samples, which proves that the replacement of nutrients and metabolites between the intestinal flora and the host through the continuous membrane transportation function, so as to provide the material transportation basis for the intestinal microorganisms to help the host digest food and provide vitamins and amino acids. According to the results of the KEGG metabolic pathway annotations, we acquire the gene function (Fig.5).

### Fig. 4 Relative abundance of pathways

### Fig. 5 KEGG pathway annotation

## CAZy annotation results

Comparing the Unique Genes with CAZy (carbohydrate enzyme professional database) database, the number of genes corresponding to the six carbohydrate enzymes was obtained, as shown in figure 3, the GH (Glycoside hydrolases) corresponding to the maximum proportion of genes, PL (Polysaccharide lyases) corresponding to the minimum number of genes. According to the results of the annotation to draw the samples six carbohydrate enzyme relative abundance bar chart (Fig. 6) and number of matched genes of carbohydrates (Fig. 7).

### Fig. 6 Relative abundance of carbohydrates

### Fig. 7 Number of matched genes of carbohydrates

## EggNOG annotates

EggNOG database combines COG, KOG and Orthologous Groups function database, mainly through the known protein to get corresponding functional annotation of the sequences, comparing the Unique Genes with eggNOG database, the main function of genes including gene replication, repair of amino acid

transport and metabolism of carbohydrates, such as transport and metabolism, eggNOG database annotation results below (Fig. 8 and Fig. 9).

Fig. 8 Relative abundance of function class

Fig. 9 Number of matched genes of function class

## Resistant gene annotation

To reflect the distribution of ARO in each sample, according to the abundance information of ARO in each sample, the top 30 aros were selected to draw the abundance cluster heat map, and the results were shown as follows (Fig.10). According to the annotation results of CARD database, the analysis circle of species belonging of resistance genes was drawn (Fig. 11).

**Figure.10** ARO distribution and abundance cluster heat map. The right vertical axis is the ARO name, and the left vertical axis is the ARO cluster tree.

## Discussion

The dominant phyla in the human and mouse gut were *Firmicutes* and *Bacteroidetes* (Consortium 2012), and the four most abundant bacterial phyla were *Firmicutes*, *Proteobacteria*, *Bacteroidetes* and *Actinobacteria* in chickens (Choi et al. 2014). *Firmicutes* and *Bacteroidetes* were the two most prevalent bacteria phyla found in the ruminant gastrointestinal tract (Ye et al. 2016). The two most common and abundant bacteria phyla among fish, were *Proteobacteria* and *Fusobacteria* (Hill et al. 2016; Wong and Rawls 2012). For invertebrates, *Proteobacteria* and *Firmicutes* were the dominant phylum among *Drosophila melanogaster* gut bacterial communities (Broderick and Lemaitre 2012), and *Proteobacteria* as the dominant phylum in *E.sinensis* (Chen et al. 2015). The results from this study show that *Proteobacteria* and *Firmicutes* are the dominant bacteria of sable intestinal microorganisms at the phylum level. Although the abundant gut bacterial under phyla level are similar, but with significantly different abundances. Demonstrating that dominant species in the phyla *Bacteroidetes*, *Tenericutes*, *Proteobacteria* and *Firmicutes* closely related to the host. Our studies support the view there are evolutionary relationships between these animals.

According to KEGG annotation results, the number of genes corresponding to metabolism function reached 77,891, accounting for 60.93% of the total number of genes. The highest number of genes related to carbohydrate catabolism was 15,397, accounting for 11.86%, indicating that the bacterial community is closely related to digestive tract function. At the order level, *Enterobacteriales*, *Lactobacillales* and *Clostridiales* were the dominant bacterial community, demonstrating that the intestinal flora plays a significant role in carbohydrate metabolism, the dominant order of *Firmicutes* in

the intestinal microorganisms, *Clostridium*, mainly attributed to the decomposition of cellulose, and some carbohydrates catabolism and vitamin synthesis are usually performed by the intestinal flora (Gao et al. 2020). After CAZy database annotation, the number of genes corresponding to Glycoside hydrolases was 5267. Glycoside hydrolases are mainly composed of glycoconjugates and glycoconjugates. The corresponding number of Glycosyltransferase genes were 3,347, the main function is to attach the activated sugar groups to different receptor molecules. The corresponding number of Carbohydrate-binding modules genes were 1,421, the corresponding number of Carbohydrate Esterases genes were 542, the number of Polysaccharide lysates corresponding genes were 51, the corresponding number of genes in Auxiliary activities were 174. These enzymes complete the degradation and modification of carbohydrates and the formation of glycosidic bonds. Recently, plenty of researches has aimed to determine the complexity of the relationship between the host and the gut microbiota. Although the intestinal microbe is closely linked to the immune system, their relationship with gut immunity remains unknown. Intestinal flora plays an important role in maintaining intestinal health. In this study, based on sequence alignment in non-redundant CARD databases, according to the results of the annotation found the abundant multiple drug-resistant Mexb protein genes, indicating that the gut microflora plays an effective role in the immune reactions on exogenous substances. Among the functions of Environmental information processing, the number of genes related to membrane transport was the highest, accounting for 7.79% of the total genes of all samples, it indicates that the host and intestinal flora are constantly exchanging substances. Inorganic transport and metabolism consisted phosphate, sulfate, and various cation transporters (Gill et al. 2006). The relevant microbial proteins identified were featured into COG functional database, there is high level gene expression in inorganic transport and metabolism of healthy children, obese children with non-alcoholic fatty liver disease does the opposite (Michail et al. 2014). The cell wall/membrane/envelope biogenesis genes participate in transmembrane transport and the exocytosis of antibiotics to resist the effects of tetracycline hydrochloride, indicating that gut microbiota can enhance antibiotic resistance capability. Hence, opportunistic microorganism can survive in the mouse gut. The numbers of genes related to genetic information processing, such as gene replication, transcription, translation and repair, was 14,859, accounting for 11.62 percent of the total genes. According to annotation results, there are a large number of genes related to host diseases in intestinal flora, with the number of genes reaching 8167, accounting for 6.39%. Innate immunity is the significant host defense mechanism which lacks the high selection mechanisms of adaptive immunity. This result is consistent with our findings. Interestingly, TLRs were expressed at low levels in the gut of *Drosophila melanogaster*. Many researches have shown that the correlation between the microbiological compositions and inflammatory parameters can serve as a biological indicator to evaluate the occurrence of diseases. *Lactobacillaceae* and *Enterobacteriaceae* as the dominant bacteria at the family level, they play important roles in assisting the host to break down carbohydrates and ferment sugars to maintain the host nutrition metabolism. Through further analysis at the genus level, *Lactobacillus* and *Escherichia* have high abundance, *Lactobacillus*, as a beneficial bacterium, act as a barrier to foreign invaders, inhibit the growth of other pathogenic bacteria and synthetic vitamins and amino acids for host, maintaining the dynamic balance of gut microbes, also it plays an important role in tumor inhibition, in some hosts with disease, there may be a decrease in *Lactobacillus* in the gut. There are also genes

regulating cell processes in intestinal flora, among which the number of genes regulating cell growth and apoptosis is 1324, accounting for 1.04%. The number of genes regulating cell movement was 1336, accounting for 1.05%. The number of genes regulating the cell community was 3,542, accounting for 2.77%. The number of genes regulating the transport and catabolism of cells was 1004, accounting for 0.79%. The number of genes related to the biological system was 3849, accounting for 3.01% of the total genes. In this function, the number of genes related to the endocrine system was up to 1372, accounting for 1.07%. In this study, we identify the complex microbial population structure of sables based on metagenomic sequencing method, which uses the whole metagenomic data, mapping the sequences to the known genes or the pathways in the existing databases, such as CAZy, KEGG, or eggNOG, and then exploring the genetic composition and functional diversity of microbial community based on the mapped functional categories.

## **Declarations**

## **Ethics approval and consent to participate**

This work was carried out in compliance with the current laws in China.

## **Consent for publication**

The written informed consent forms were taken from the volunteers.

## **Availability of data and materials**

All the raw sequences were submitted to the NCBI Sequence Read Archive, under Accession Number SRP265006.

## **Competing interests**

The authors declare that they have no competing interests.

## **Funding**

the National Natural Science Fund of China

## **Authors' contributions**

All authors have contributed to this research work. All authors read and approved the final manuscript.

## Acknowledgements

We are grateful for support from the National Natural Science Foundation of China.

## References

Antunes KH, Fachi JL, de Paula R, da Silva EF, Pral LP, dos Santos AÁ, Dias GBM, Vargas JE, Puga R, Mayer FQ, Maito F, Zárata-Bladés CR, Ajami NJ, Sant'Ana MR, Candreva T, Rodrigues HG, Schmiele M, Silva Clerici MTP, Proença-Modena JL, Vieira AT, Mackay CR, Mansur D, Caballero MT, Marzec J, Li J, Wang X, Bell D, Polack FP, Kleeberger SR, Stein RT, Vinolo MAR, de Souza APD (2019) Microbiota-derived acetate protects against respiratory syncytial virus infection through a GPR43-type 1 interferon response. *Nature Communications* 10(1):3273. <https://doi.org/10.1038/s41467-019-11152-6>

Bang S-J, Kim G, Lim MY, Song E-J, Jung D-H, Kum J-S, Nam Y-D, Park C-S, Seo D-H (2018) The influence of in vitro pectin fermentation on the human fecal microbiome. *AMB Express* 8(1):98. <https://doi.org/10.1186/s13568-018-0629-9>

Blakeley-Ruiz JA, Erickson AR, Cantarel BL, Xiong W, Adams R, Jansson JK, Fraser CM, Hettich RL (2019) Metaproteomics reveals persistent and phylum-redundant metabolic functional stability in adult human gut microbiomes of Crohn's remission patients despite temporal variations in microbial taxa, genomes, and proteomes. *Microbiome* 7(1):18. <https://doi.org/10.1186/s40168-019-0631-8>

Broderick NA, Lemaitre B (2012) Gut-associated microbes of *Drosophila melanogaster*. *Gut Microbes* 3(4):307-321. <https://doi.org/10.4161/gmic.19896>

Brum J, Ignacio Espinoza JC, Roux S, Doucier G, Acinas S, Alberti A, Chaffron S, Cruaud C, de Vargas C, Gasol J, Gorsky G, Gregory A, Guidi L, Hingamp P, Iudicone D, Not F, Ogata H, Pesant S, Poulos B, Sullivan M (2015) Ocean plankton. Patterns and ecological drivers of ocean viral communities. *Science* 348 <https://doi.org/10.1126/science.1261498>

Buchfink B, Xie C, Huson DH (2015) Fast and sensitive protein alignment using DIAMOND. *Nature Methods* 12(1):59-60. <https://doi.org/10.1038/nmeth.3176>

Chen X, Di P, Wang H, Li B, Pan Y, Yan S, Wang Y (2015) Bacterial Community Associated with the Intestinal Tract of Chinese Mitten Crab (*Eriocheir sinensis*) Farmed in Lake Tai, China. *PLOS ONE* 10(4):e0123990. <https://doi.org/10.1371/journal.pone.0123990>

Choi JH, Kim GB, Cha CJ (2014) Spatial heterogeneity and stability of bacterial community in the gastrointestinal tracts of broiler chickens. *Poultry Science* 93(8):1942-1950. <http://www.sciencedirect.com/science/article/pii/S0032579119384640>

Consortium (2012) Structure, function and diversity of the healthy human microbiome. *Nature* 486(7402):207-214. <https://doi.org/10.1038/nature11234>

De Mandal S, Singh SS, Muthukumaran RB, Thanzami K, Kumar V, Kumar NS (2018) Metagenomic analysis and the functional profiles of traditional fermented pork fat 'sa-um' of Northeast India. *AMB Express* 8(1):163. <https://doi.org/10.1186/s13568-018-0695-z>

Deng Y, Cheng C, Xie J, Liu S, Ma H, Feng J, Su Y, Guo Z (2019) Coupled changes of bacterial community and function in the gut of mud crab (*Scylla Paramamosain*) in response to Baimang disease. *AMB Express* 9(1):18. <https://doi.org/10.1186/s13568-019-0745-1>

Dong J, Li X, Zhang R, Zhao Y, Wu G, Liu J, Zhu X, Li L (2018) Comparative analysis of the intestinal bacterial community and expression of gut immunity genes in the Chinese Mitten Crab (*Eriocheir sinensis*). *AMB Express* 8(1):192. <https://doi.org/10.1186/s13568-018-0722-0>

Doulberis M, Angelopoulou K, Kaldrymidou E, Tsingotjidou A, Abas Z, Erdman SE, Poutahidis T (2015) Cholera-toxin suppresses carcinogenesis in a mouse model of inflammation-driven sporadic colon cancer. *Carcinogenesis* 36(2):280-290. <https://doi.org/10.1093/carcin/bgu325>

Federici M (2019) Gut microbiome and microbial metabolites: a new system affecting metabolic disorders. *Journal of Endocrinological Investigation* <https://doi.org/10.1007/s40618-019-01022-9>

Feng Q, Liang S, Jia H, Stadlmayr A, Tang L, Lan Z, Zhang D, Xia H, Xu X, Jie Z, Su L, Li X, Li X, Li J, Xiao L, Huber-Schönauer U, Niederseer D, Xu X, Al-Aama JY, Yang H, Wang J, Kristiansen K, Arumugam M, Tilg H, Datz C, Wang J (2015) Gut microbiome development along the colorectal adenoma–carcinoma sequence. *Nature Communications* 6(1):6528. <https://doi.org/10.1038/ncomms7528>

Gao Y, Yang L, Chin Y, Liu F, Li RW, Yuan S, Xue C, Xu J, Tang Q (2020) Astaxanthin n-Octanoic Acid Diester Ameliorates Insulin Resistance and Modulates Gut Microbiota in High-Fat and High-Sucrose Diet-Fed Mice. *Int J Mol Sci* 21(6):2149. <https://doi.org/10.3390/ijms21062149>

Gill SR, Pop M, Deboy RT, Eckburg PB, Turnbaugh PJ, Samuel BS, Gordon JI, Relman DA, Fraser-Liggett CM, Nelson KE (2006) Metagenomic analysis of the human distal gut microbiome. *Science* 312(5778):1355-1359. <https://doi.org/10.1126/science.1124234>

Grieneisen LE, Charpentier MJE, Alberts SC, Blekhman R, Bradburd G, Tung J, Archie EA (2019) Genes, geology and germs: gut microbiota across a primate hybrid zone are explained by site soil properties, not host species. *Proc Biol Sci* 286(1901):20190431-20190431. <https://doi.org/10.1098/rspb.2019.0431>

Guan Y, Zhang H, Gao X, Shang S, Wu X, Chen J, Zhang W, Zhang W, Jiang M, Zhang B, Chen P (2016) Comparison of the bacterial communities in feces from wild versus housed sables (*Martes zibellina*) by high-throughput sequence analysis of the bacterial 16S rRNA gene. *AMB Express* 6(1):98-98. <https://doi.org/10.1186/s13568-016-0254-4>

- Hale VL, Tan CL, Niu K, Yang Y, Zhang Q, Knight R, Amato KR (2019) Gut microbiota in wild and captive Guizhou snub-nosed monkeys, *Rhinopithecus brelichi*. *American Journal of Primatology* 81(10-11):e22989. <https://doi.org/10.1002/ajp.22989>
- Hasan AU, Rahman A, Kobori H (2019) Interactions between Host PPARs and Gut Microbiota in Health and Disease. *Int J Mol Sci* 20(2):387. <https://pubmed.ncbi.nlm.nih.gov/30658440>
- Hill JH, Franzosa EA, Huttenhower C, Guillemin K (2016) A conserved bacterial protein induces pancreatic beta cell expansion during zebrafish development. *Elife* 5:e20145. <https://doi.org/10.1101/j.1365-294x.2012.05646.x>
- Huson D, Mitra S, Ruscheweyh H-J, Weber N, Schuster S (2011) Integrative Analysis of Environmental Sequences Using MEGAN4. *Genome research* 21:1552-60. <https://doi.org/10.1101/gr.120618.111>
- Jain A, Li XH, Chen WN (2018) Similarities and differences in gut microbiome composition correlate with dietary patterns of Indian and Chinese adults. *AMB Express* 8(1):104. <https://doi.org/10.1186/s13568-018-0632-1>
- Jang S-E, Jeong J-J, Kim J-K, Han MJ, Kim D-H (2018) Simultaneous Amelioration of Colitis and Liver Injury in Mice by *Bifidobacterium longum* LC67 and *Lactobacillus plantarum* LC27. *Scientific reports* 8(1):7500-7500. <https://doi.org/10.1038/s41598-018-25775-0>
- Johnson G (2019) High throughput DNA extraction of legume root nodules for rhizobial metagenomics. *AMB Express* 9(1):47. <https://doi.org/10.1186/s13568-019-0771-z>
- Karlsson FH, Tremaroli V, Nookaew I, Bergström G, Behre CJ, Fagerberg B, Nielsen J, Bäckhed F (2013) Gut metagenome in European women with normal, impaired and diabetic glucose control. *Nature* 498(7452):99-103. <https://doi.org/10.1038/nature12198>
- Krone CL, Biesbroek G, Trzciński K, Sanders EAM, Bogaert D (2014) Respiratory Microbiota Dynamics following *Streptococcus pneumoniae* Acquisition in Young and Elderly Mice *Infect Immun* 82(4):1725. <http://iai.asm.org/content/82/4/1725.abstract>
- Li B, Malyarchuk B, Ma Z, Derenko M, Zhao J, Zhou X (2013) Phylogeography of sable (*Martes zibellina* L. 1758) in the southeast portion of its range based on mitochondrial DNA variation: Highlighting the evolutionary history of the sable. *Acta Theriologica* 58 <https://doi.org/10.1007/s13364-012-0100-2>
- Li J, Jia H, Cai X, Zhong H, Feng Q, Sunagawa S, Arumugam M, Kultima JR, Prifti E, Nielsen T, Juncker AS, Manichanh C, Chen B, Zhang W, Levenez F, Wang J, Xu X, Xiao L, Liang S, Zhang D, Zhang Z, Chen W, Zhao H, Al-Aama JY, Edris S, Yang H, Wang J, Hansen T, Nielsen HB, Brunak S, Kristiansen K, Guarner F, Pedersen O, Doré J, Ehrlich SD, Pons N, Le Chatelier E, Batto J-M, Kennedy S, Haimet F, Winogradski Y, Pelletier E, LePaslier D, Artiguenave F, Bruls T, Weissenbach J, Turner K, Parkhill J, Antolin M, Casellas F, Borruel N, Varela E, Torrejon A, Denariáz G, Derrien M, van Hylckama Vlieg JET, Viega P, Oozeer R, Knoll J,

Rescigno M, Brechot C, M'Rini C, Mérieux A, Yamada T, Tims S, Zoetendal EG, Kleerebezem M, de Vos WM, Cultrone A, Leclerc M, Juste C, Guedon E, Delorme C, Layec S, Khaci G, van de Guchte M, Vandemeulebrouck G, Jamet A, Dervyn R, Sanchez N, Blottière H, Maguin E, Renault P, Tap J, Mende DR, Bork P, Wang J, Meta HITC (2014) An integrated catalog of reference genes in the human gut microbiome. *Nature Biotechnology* 32(8):834-841. <https://doi.org/10.1038/nbt.2942>

Li S, Wang Z, Yang Y, Yang S, Yao C, Liu K, Cui S, Zou Q, Sun H, Guo G (2017) *Lachnospiraceae* shift in the microbial community of mice faecal sample effects on water immersion restraint stress. *AMB Express* 7(1):82. <https://doi.org/10.1186/s13568-017-0383-4>

Li X, Liang S, Xia Z, Qu J, Liu H, Liu C, Yang H, Wang J, Madsen L, Hou Y, Li J, Jia H, Kristiansen K, Xiao L (2018a) Establishment of a *Macaca fascicularis* gut microbiome gene catalog and comparison with the human, pig, and mouse gut microbiomes. *GigaScience* 7(9) <https://doi.org/10.1093/gigascience/giy100>

Li X, Yin J, Zhu Y, Wang X, Hu X, Bao W, Huang Y, Chen L, Chen S, Yang W, Shan Z, Liu L (2018b) Effects of Whole Milk Supplementation on Gut Microbiota and Cardiometabolic Biomarkers in Subjects with and without Lactose Malabsorption. *Nutrients* 10(10):1403. <https://doi.org/10.3390/nu10101403>

Li Z, Si H, Nan W, Wang X, Zhang T, Li G (2019) Bacterial community and metabolome shifts in the cecum and colon of captive sika deer (*Cervus nippon*) from birth to post weaning. *FEMS Microbiology Letters* 366(4) <https://doi.org/10.1093/femsle/fnz010>

Liu Y, Zheng Z, Yu L, Wu S, Sun L, Wu S, Xu Q, Cai S, Qin N, Bao W (2019) Examination of the temporal and spatial dynamics of the gut microbiome in newborn piglets reveals distinct microbial communities in six intestinal segments. *Scientific Reports* 9(1):3453. <https://doi.org/10.1038/s41598-019-40235-z>

Luo R, Liu B, Xie Y, Li Z, Huang W, Yuan J, He G, Chen Y, Pan Q, Liu Y, Tang J, Wu G, Zhang H, Shi Y, Liu Y, Yu C, Wang B, Lu Y, Han C, Cheung DW, Yiu S-M, Peng S, Xiaoqian Z, Liu G, Liao X, Li Y, Yang H, Wang J, Lam T-W, Wang J (2012) SOAPdenovo2: an empirically improved memory-efficient short-read de novo assembler. *GigaScience* 1(1):18. <https://doi.org/10.1186/2047-217X-1-18>

Ma C, Chen C, Jia L, He X, Zhang B (2019) Comparison of the intestinal microbiota composition and function in healthy and diseased Yunlong Grouper. *AMB Express* 9(1):187. <https://doi.org/10.1186/s13568-019-0913-3>

Martin TC, Visconti A, Spector TD, Falchi M (2018) Conducting metagenomic studies in microbiology and clinical research. *Applied Microbiology Biotechnology* 102(20):8629-8646. <https://doi.org/10.1007/s00253-018-9209-9>

Mende D, Waller A, Sunagawa S, Järvelin A, Chan M, Arumugam M, Raes J, Bork P (2012) Assessment of Metagenomic Assembly Using Simulated Next Generation Sequencing Data. *PloS one* 7:e31386. <https://doi.org/10.1371/journal.pone.0031386>

Michail S, Lin M, Frey MR, Fanter R, Paliy O, Hilbush B, Reo NV (2014) Altered gut microbial energy and metabolism in children with non-alcoholic fatty liver disease. *FEMS Microbiology Ecology* 91(2):1-9.  
<https://doi.org/10.1093/femsec/fiu002>

Monakhov VG, Modorov MV, Ranyuk MN (2018) Genetic Effects of Sable (*Martes zibellina* L.) Reintroduction in Western Siberia. *Russian Journal of Genetics* 54(3):358-362.  
<https://doi.org/10.1134/S1022795418030079>

Mustonen A-M, Nieminen P (2006) Fatty acid composition in the central and peripheral adipose tissues of the sable (*Martes zibellina*). *Journal of Thermal Biology* 31:617-625.  
<https://doi.org/10.1016/j.jtherbio.2006.08.004>

Mustonen A-M, Puukka M, Seppo S, Paakkonen T, Aho J, Nieminen P (2006) Adaptations to fasting in a terrestrial mustelid, the sable (*Martes zibellina*). *Comparative biochemistry and physiology Part A, Molecular & integrative physiology* 144:444-50. <https://doi.org/10.1016/j.cbpa.2006.03.008>

Oliphant K, Allen-Vercoe E (2019) Macronutrient metabolism by the human gut microbiome: major fermentation by-products and their impact on host health. *Microbiome* 7(1):91.  
<https://doi.org/10.1186/s40168-019-0704-8>

Pan J, Yin J, Zhang K, Xie P, Ding H, Huang X, Blachier F, Kong X (2019) Dietary xylo-oligosaccharide supplementation alters gut microbial composition and activity in pigs according to age and dose. *AMB Express* 9(1):134. <https://doi.org/10.1186/s13568-019-0858-6>

Pekkala S, Lensu S, Nokia M, Vanhatalo S, Koch LG, Britton SL, Kainulainen H (2017) Intrinsic aerobic capacity governs the associations between gut microbiota composition and fat metabolism age-dependently in rat siblings. *Physiological Genomics* 49(12):733-746.  
<https://doi.org/10.1152/physiolgenomics.00081.2017>

Qin J, Li R, Raes J, Arumugam M, Burgdorf KS, Manichanh C, Nielsen T, Pons N, Levenez F, Yamada T, Mende DR, Li J, Xu J, Li S, Li D, Cao J, Wang B, Liang H, Zheng H, Xie Y, Tap J, Lepage P, Bertalan M, Batto J-M, Hansen T, Le Paslier D, Linneberg A, Nielsen HB, Pelletier E, Renault P, Sicheritz-Ponten T, Turner K, Zhu H, Yu C, Li S, Jian M, Zhou Y, Li Y, Zhang X, Li S, Qin N, Yang H, Wang J, Brunak S, Doré J, Guarner F, Kristiansen K, Pedersen O, Parkhill J, Weissenbach J, Antolin M, Artiguenave F, Blottiere H, Borruel N, Bruls T, Casellas F, Chervaux C, Cultrone A, Delorme C, Denariáz G, Dervyn R, Forte M, Friss C, van de Guchte M, Guedon E, Haimet F, Jamet A, Juste C, Kaci G, Kleerebezem M, Knol J, Kristensen M, Layec S, Le Roux K, Leclerc M, Maguin E, Melo Minardi R, Oozeer R, Rescigno M, Sanchez N, Tims S, Torrejon T, Varela E, de Vos W, Winogradsky Y, Zoetendal E, Bork P, Ehrlich SD, Wang J, Meta HITC (2010) A human gut microbial gene catalogue established by metagenomic sequencing. *Nature* 464(7285):59-65.  
<https://doi.org/10.1038/nature08821>

Qin J, Li Y, Cai Z, Li S, Zhu J, Zhang F, Liang S, Zhang W, Guan Y, Shen D, Peng Y, Zhang D, Jie Z, Wu W, Qin Y, Xue W, Li J, Han L, Lu D, Wu P, Dai Y, Sun X, Li Z, Tang A, Zhong S, Li X, Chen W, Xu R, Wang M, Feng

Q, Gong M, Yu J, Zhang Y, Zhang M, Hansen T, Sanchez G, Raes J, Falony G, Okuda S, Almeida M, LeChatelier E, Renault P, Pons N, Batto J-M, Zhang Z, Chen H, Yang R, Zheng W, Li S, Yang H, Wang J, Ehrlich SD, Nielsen R, Pedersen O, Kristiansen K, Wang J (2012) A metagenome-wide association study of gut microbiota in type 2 diabetes. *Nature* 490(7418):55-60. <https://doi.org/10.1038/nature11450>

Qin N, Yang F, Li A, Prifti E, Chen Y, Shao L, Guo J, Le Chatelier E, Yao J, Wu L, Zhou J, Ni S, Liu L, Pons N, Batto JM, Kennedy SP, Leonard P, Yuan C, Ding W, Chen Y, Hu X, Zheng B, Qian G, Xu W, Ehrlich SD, Zheng S, Li L (2014) Alterations of the human gut microbiome in liver cirrhosis. *Nature* 513:59. <https://doi.org/10.1038/nature13568>

Robertson RC, Kaliannan K, Strain CR, Ross RP, Stanton C, Kang JX (2018) Maternal omega-3 fatty acids regulate offspring obesity through persistent modulation of gut microbiota. *Microbiome* 6(1):95. <https://doi.org/10.1186/s40168-018-0476-6>

Scher JU, Sczesnak A, Longman RS, Segata N, Ubeda C, Bielski C, Rostron T, Cerundolo V, Pamer EG, Abramson SB, Huttenhower C, Littman DR (2013) Expansion of intestinal *Prevotella copri* correlates with enhanced susceptibility to arthritis. *Elife* 2:e01202-e01202. <https://doi.org/10.7554/eLife.01202.001>

Shui Y, Guan Z-B, Liu G-F, Fan L-M (2020) Gut microbiota of red swamp crayfish *Procambarus clarkii* in integrated crayfish-rice cultivation model. *AMB Express* 10(1):5. <https://doi.org/10.1186/s13568-019-0944-9>

Si J, Feng L, Gao J, Huang Y, Zhang G, Mo J, Zhu S, Qi W, Liang J, Lan G (2020) Evaluating the association between feed efficiency and the fecal microbiota of early-life Duroc pigs using 16S rRNA sequencing. *AMB Express* 10(1):115. <https://doi.org/10.1186/s13568-020-01050-2>

Srugo SA, Bloise E, Nguyen TT-TN, Connor KL (2019) Impact of Maternal Malnutrition on Gut Barrier Defense: Implications for Pregnancy Health and Fetal Development. *Nutrients* 11(6):1375. <https://doi.org/10.3390/nu11061375>

Svishcheva GR, Kashtanov SN (2011) Reproductive strategy of the sable (*Martes zibellina* Linnaeus, 1758): An analysis of litter size inheritance in farm-raised populations. *Russian Journal of Genetics: Applied Research* 1(3):221-225. <https://doi.org/10.1134/S2079059711030129>

Taha-Abdelaziz K, Yitbarek A, Alkie TN, Hodgins DC, Read LR, Weese JS, Sharif S (2018) PLGA-encapsulated CpG ODN and *Campylobacter jejuni* lysate modulate cecal microbiota composition in broiler chickens experimentally challenged with *C. jejuni*. *Scientific Reports* 8(1):12076. <https://doi.org/10.1038/s41598-018-30510-w>

Tully BJ, Graham ED, Heidelberg JF (2018) The reconstruction of 2,631 draft metagenome-assembled genomes from the global oceans. *Scientific Data* 5:170203. <https://doi.org/10.1038/sdata.2017.203>

Villar E, Farrant GK, Follows M, Garczarek L, Speich S, Audic S, Bittner L, Blanke B, Brum JR, Brunet C, Casotti R, Chase A, Dolan JR, d'Ortenzio F, Gattuso J-P, Grima N, Guidi L, Hill CN, Jahn O, Jamet J-L, Le Goff H, Lepoivre C, Malviya S, Pelletier E, Romagnan J-B, Roux S, Santini S, Scalco E, Schwenck SM, Tanaka A, Testor P, Vannier T, Vincent F, Zingone A, Dimier C, Picheral M, Searson S, Kandels-Lewis S, Acinas SG, Bork P, Boss E, de Vargas C, Gorsky G, Ogata H, Pesant S, Sullivan MB, Sunagawa S, Wincker P, Karsenti E, Bowler C, Not F, Hingamp P, Ludicone D (2015) Environmental characteristics of Agulhas rings affect interocean plankton transport. *Science* 348(6237):1261447.

<https://science.sciencemag.org/content/sci/348/6237/1261447.full.pdf>

Wong S, Rawls JF (2012) Intestinal microbiota composition in fishes is influenced by host ecology and environment. *Mol Ecol* 21(13):3100-3102. <https://doi.org/10.1111/j.1365-294x.2012.05646.x>

Wu Q, Wang X, Ding Y, Hu Y, Nie Y, Wei W, Ma S, Yan L, Zhu L, Wei F (2017a) Seasonal variation in nutrient utilization shapes gut microbiome structure and function in wild giant pandas. *Proc Biol Sci* 284(1862):20170955. <https://doi.org/10.1098/rspb.2017.0955>

Wu X, Zhang H, Chen J, Shang S, Yan J, Chen Y, Tang X, Zhang H (2017b) Analysis and comparison of the wolf microbiome under different environmental factors using three different data of Next Generation Sequencing. *Scientific Reports* 7(1):11332. <https://doi.org/10.1038/s41598-017-11770-4>

Xu C, Liu J, Gao J, Wu X, Cui C, Wei H, Zheng R, Peng J (2020) Combined Soluble Fiber-Mediated Intestinal Microbiota Improve Insulin Sensitivity of Obese Mice. *Nutrients* 12(2):351. <https://doi.org/10.3390/nu12020351>

Xue Z, Zhang J, Zhang R, Huang Z, Wan Q, Zhang Z (2019) Comparative analysis of gut bacterial communities in housefly larvae fed different diets using a high-throughput sequencing approach. *FEMS Microbiology Letters* 366(11) <https://doi.org/10.1093/femsle/fnz126>

Ye H, Liu J, Feng P, Zhu W, Mao S (2016) Grain-rich diets altered the colonic fermentation and mucosa-associated bacterial communities and induced mucosal injuries in goats. *Scientific reports* 6:20329-20329. <https://doi.org/10.1038/srep20329>

Zeller G, Tap J, Voigt A, Sunagawa S, Kultima J, Costea P, Amiot A, Böhm J, Brunetti F, Habermann N, Hercog R, Koch M, Luciani A, Mende D, Schneider M, Schrotz-King P, Tournigand C, Tran Van Nhieu J, Yamada T, Bork P (2014) Potential of fecal microbiota for early-stage detection of colorectal cancer. *Molecular Systems Biology* 10 <https://doi.org/10.15252/msb.20145645>

Zhu H, Zeng D, Wang N, Niu L-l, Zhou Y, Zeng Y, Ni X-q (2018) Microbial community and diversity in the feces of Sichuan takin (*Budorcas taxicolor tibetana*) as revealed by Illumina Miseq sequencing and quantitative real-time PCR. *AMB Express* 8(1):68. <https://doi.org/10.1186/s13568-018-0599-y>

# Figures

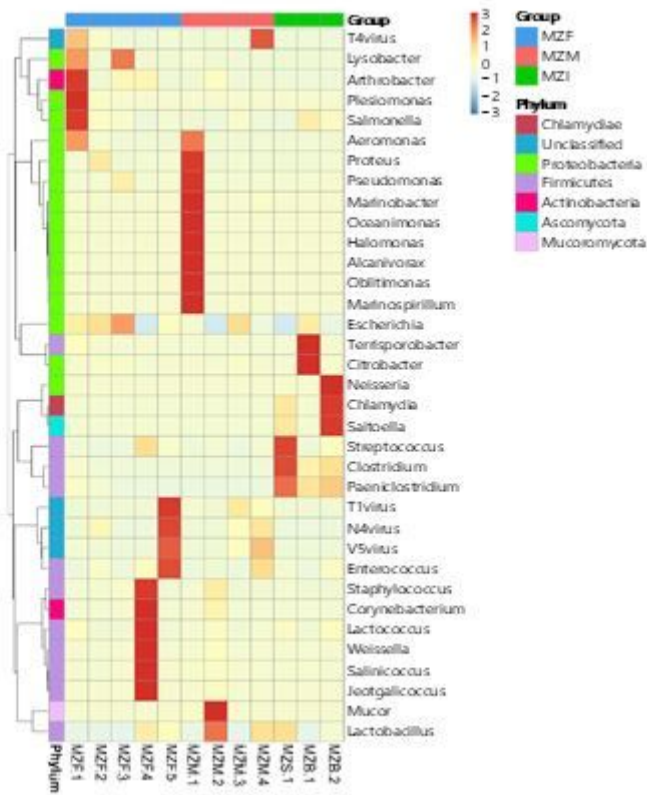


Figure 1

Cluster heat map of relative abundance at genus level

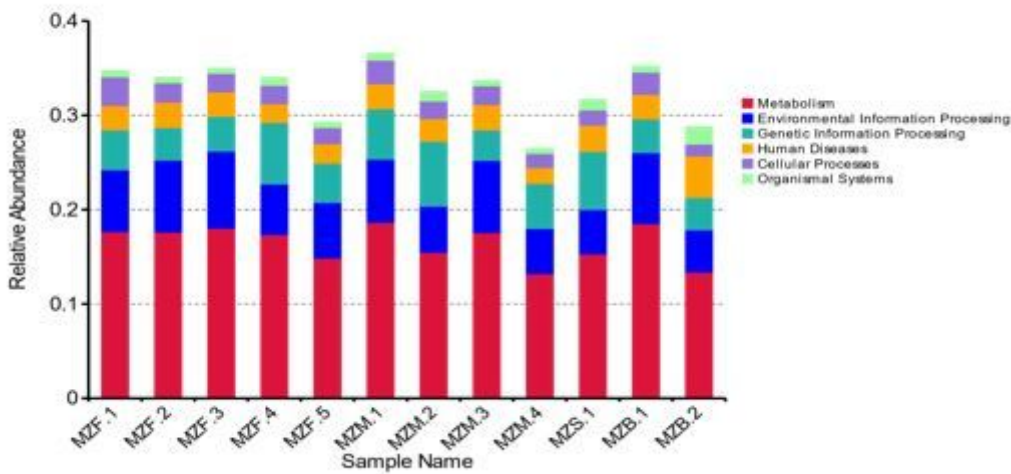


Figure 2

Relative abundance of pathways

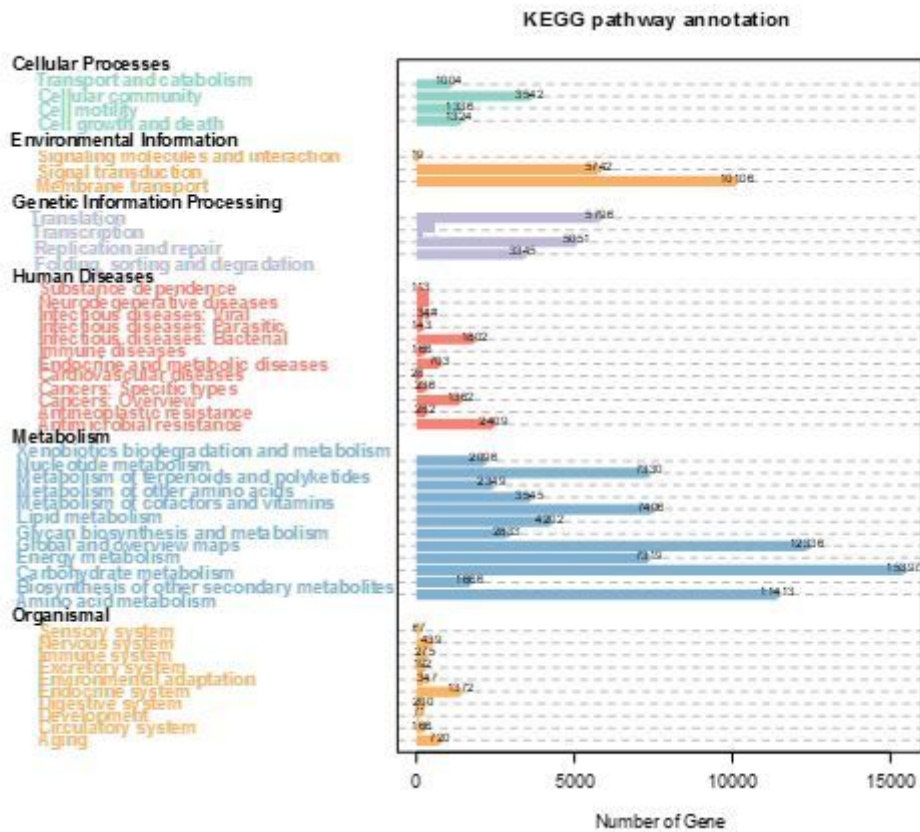


Figure 3

KEGG pathway annotation

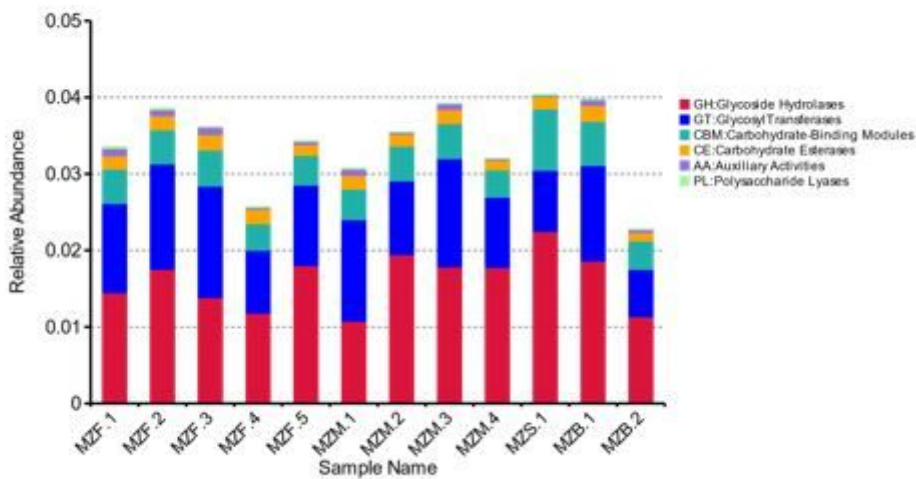


Figure 4

Relative abundance of carbohydrates

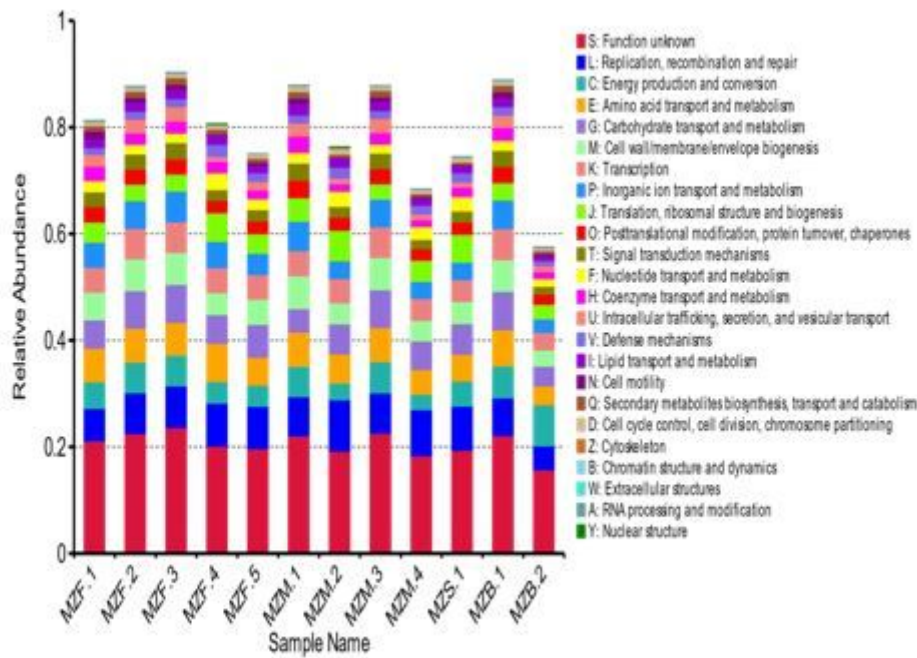


Figure 5

Relative abundance of function class

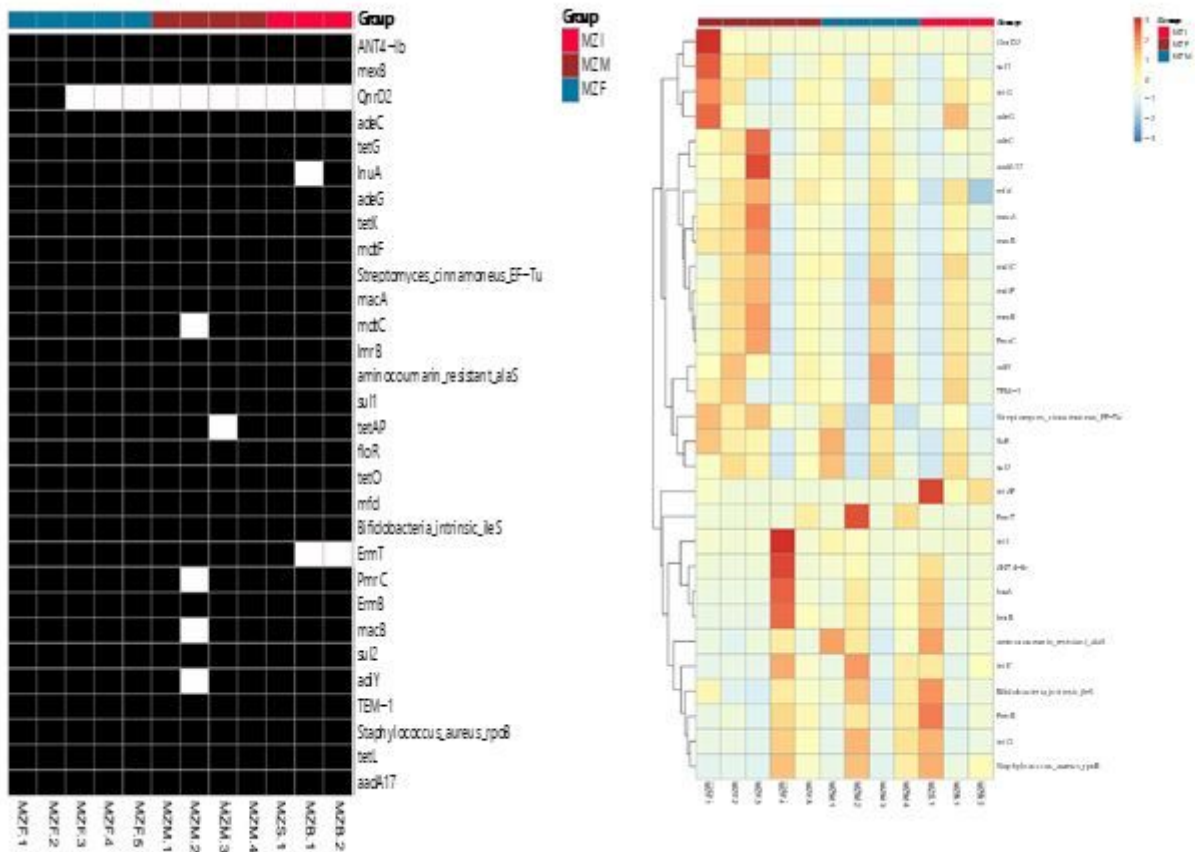
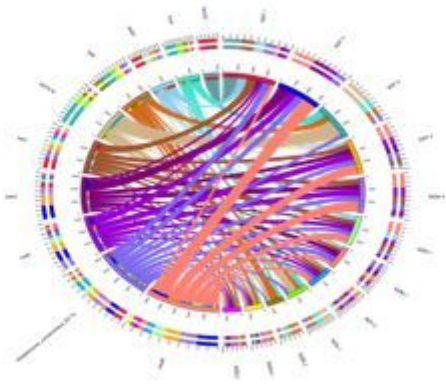


Figure 6

ARO distribution and abundance cluster heat map A) is the heat map of ARO distribution. The horizontal axis is the name of the sample, and the right vertical axis is the name of ARO of the resistance gene type. B) is the ARO abundance cluster heat map. The right vertical axis is the ARO name, and the left vertical axis is the ARO cluster tree.



**Figure 7**

The overview circle graph of resistance gene